JPE 14-4-20

http://dx.doi.org/10.6113/JPE.2014.14.4.806
ISSN(Print): 1598-2092 / ISSN(Online): 2093-4718

Scattering Parameter-based Measurement of Planar EMI filter

Shishan Wang†, Min Gong*, and Chenchen Xu*

†*Jiangsu Key Laboratory of New Energy Generation and Power conversion, Nanjing University of Aeronautics and Astronautics, Nanjing, China

Abstract

Planar electromagnetic interference (EMI) filters are widely used to restrain the conducted EMI of switching power supplies. Such filters are characterized by small size, low parasitic parameters, and better high-frequency performance than the passive discrete EMI filter. However, EMI filter performance cannot be exactly predicted by using existing methods. Therefore, this paper proposes a method to use scattering parameters (*S*-parameters) for the measurement of EMI filter performance. A planar EMI filter sample is established. From this sample, the relationship between *S*-parameters and insertion gain (*IG*) of EMI filter is derived. To determine the *IG* under different impedances, the EMI filter is theoretically calculated and practically measured. The differential structure of the near-field coupling model is also deduced, and the *IG* is calculated under standard impedance conditions. The calculated results and actual measurements are compared to verify the feasibility of the theory.

Key words: Insertion gain (*IG*), Near-field couple, Planar EMI filter, Scattering parameter (*S*-parameter)

I. INTRODUCTION

Electromagnetic interference (EMI) is a serious problem in the development of the switching power supply and affects the normal operation of the grid and surrounding equipment [1]. According to the different interference patterns, EMI can be classified into two forms: radiated and conducted emissions. The latter is the most serious concern in power electronic systems. To meet the EMC standard, an EMI filter is often used to attenuate the conducted EMI noise. Fig. 1 shows a typical measurement setup.

Line impedance stabilization network (LISN) has been traditional used to determine the specified impedance over the working frequency range. In particular, noise can be measured when both source and load impedances are 50 Ω. An EMI filter is placed between LISN and the equipment under test (EUT), which is composed of the common mode (CM) and differential mode (DM) filters. In the EMI filter, the left DM capacitor *C*x bypasses most of the DM noise because of the low *C*x impedance. The remaining noise is blocked by the L_{DM}, which is the leakage inductance of CM inductance. The right DM capacitor *C*x bypasses most of the remaining DM currents because of the high LISN impedance. C_Y is the CM capacitor and L_{CM} is CM inductance, which constitute the CM filter used to attenuate the CM noise.

A conventional EMI filter comprises up to one-third of converter volume and weight. . To reduce the size of passive components, an integration technology that implements multiple functions into one component is proposed. The development of integration technology has made integrated EMI filters an important means to reduce the volume and weight of the whole converter. Among these integrated EMI filters, the planar EMI filter is the focus of this study. Similar to the conventional EMI filter, the planar EMI filter is composed of the CM and DM parts [2]-[4]. The core component of the planar EMI filter is an annular *inductor-capacitor* unit. To analyze the performance of the planar EMI filter and EMI noise transmission, *S*-parameters are employed [5].

The performance of EMI filters is often evaluated on the basis of insertion gain (*IG*) [6]. However, matching state is difficult to achieve in both the source and load in practical implementations. Consequently, the EMI filter is also difficult to select on the basis of the *IG* curves given by manufacturers. Therefore, the selection of the source and load impedances is important. This selection significantly affects filter performance. Notably, failing to select the appropriate

Manuscript received Jul. 22, 2013; accepted May 22, 2014
Recommended for publication by Associate Editor Tae-Woong Kim.
†Corresponding Author: Wangshishan@nuaa.edu.cn
Tel: +86-025-84890010, Nanjing Univ. of Aeronautics and Astronautics
*Jiangsu Key Laboratory of New Energy Generation and Power conversion, Nanjing University of Aeronautics and Astronautics, China

impedances will sometime magnify noise.

In the high-frequency range, the effect of near-field coupling on the EMI filter is sometimes more severe than that of the parasitic parameters of components [7]. When the near-field coupling effect of components is considered, parameter extraction becomes especially significant. Numerous extraction methods, such as the impedance and *S*-parameter methods, can be selected. However, the impedance method cannot guarantee the ideal *short-circuit* and *open-circuit* of the port, as well as the accuracy of branch and stray impedances, at high frequencies. Therefore, the *S*-parameter method is selected to extract the near-field coupling parameters while avoiding the aforementioned problems [8].

Several studies [9]-[11] have proposed methods to establish the high-frequency model on the basis of the impedance measurement method. However, ensuring that one end of the filter is a *short circuit* or *open circuit* is difficult under high frequency. In practice, model parameter accuracy is difficult to guarantee. More importantly, the existing models are unrelated, which causes problems attributed to the lack of coupling parameters. Compared with those of the filter composed of discrete components, the coupling parameters of a planar filter are more serious because all cells are integrated into a core. Therefore, the model established by using the impedance measurement method is insufficiently accurate when applied to a planar filter. For instance, literature [12] reveals that the actual insertion loss is obtained through the calculation of the minimum IL and coefficients. In fact, the IL proposed in [12] is the opposite of *IG*. However, numerous parameters are ignored in the calibration coefficient process, which causes low accuracy. Consequently, this approach has a certain application limitations.

Based on the above analysis, *S*-parameters are used to measure the characteristics of the EMI filter in this study. Combining the reflection coefficients of the noise source with the load port enables the calculation of the filter *IG*. To establish a model with enhanced high-frequency characteristics, *S*-parameters are used to measure and calculate the coupling parameters of the planar filter.

II. Measurement of Filter Characteristics by Using *S*-Parameter

A. Planar EMI Filter Structure

Applying the planar magnetic integration technology to the EMI filter and using a planar LC as a basic cell can realize the miniaturization of planar EMI filter. The basic principles of a planar EMI filter are similar to those of the discrete EMI filter (Fig. 2), both which contain the CM and DM parts. The CM module (Fig. 3) is formed by the LC unit composed of integrated inductance and capacitance. The planar LC unit

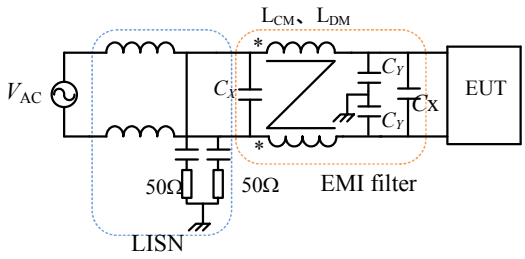

Fig. 1. Measurement setup.

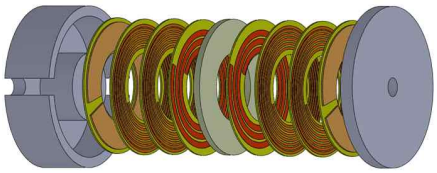

Fig. 2. Structure of planar EMI filter.

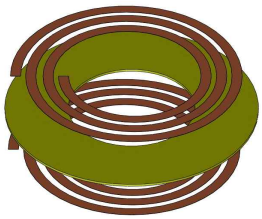

Fig. 3. Integrated unit of planar LC.

uses a high dielectric constant ceramic as the substrate. Either side of the substrate is covered with one or more turns. The DM module is composed of DM capacitance and DM inductance. When the common mode choke is not wounded tightly, it will produce leakage inductance, that is DM mode inductors.

B. S-Parameters

According to transmission line theory [13], the normalized equivalent voltage and equivalent current at any *k* port reference surface for an *n*-port network are as follows:

$$\bar{U}_k = \bar{U}_k^{+} + \bar{U}_k^{-} \tag{1}$$

$$\bar{I}_k = \bar{I}_k^{+} - \bar{I}_k^{-} \tag{2}$$

For port *k*, $\bar{U}_k^{+}$ and $\bar{I}_k^{+}$ are the normalized incident voltage and normalized incident current waves, respectively. Similarly, $\bar{U}_k^{-}$ and $\bar{I}_k^{-}$ are the normalized reflection voltage and normalized reflection current waves, respectively.

For a network characterized by *S*-parameters [14], the port impedance meets the requirements of conjugate matching. The normalized incident and reflection voltages are derived as

$$\bar{U}_k^{+} = \frac{V_k + I_k Z_k}{2\sqrt{\left|\mathrm{Re}(Z_k)\right|}} \tag{3}$$

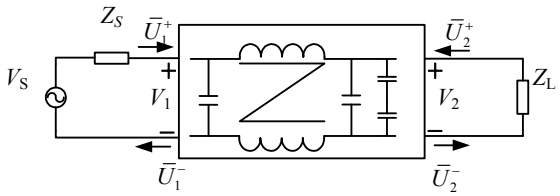

Fig. 4. Two-port microwave network model.

V_S: switch power supply noise signal
Z_S, Z_L: noise source impedance and load impedance
$\bar{U}_1^+, \bar{U}_2^+$: normalized incident voltage wave
$\bar{U}_1^-, \bar{U}_2^-$: normalized reflection voltage wave
V_1, V_2: port voltage

$$\bar{U}_k^- = \frac{V_k - I_k Z_k^*}{2\sqrt{\left|\mathrm{Re}(Z_k^*)\right|}} \tag{4}$$

In the equation, V_k, I_k are the voltage and current of the port, respectively; Z_k is the input impedance of the EMI filter; and Z_k^* is the output impedance of the filter.

Equations (1) and (2) can yield $\bar{U}_k^+, \bar{U}_k^-$ as follows:

$$\bar{U}_k^+ = (\bar{U}_k + \bar{I}_k)/2 \tag{5}$$

$$\bar{U}_k^- = (\bar{U}_k - \bar{I}_k)/2 \tag{6}$$

Transforming the k port characteristics on all ports enables the derivation matrices of the incident and reflected waves of the normalized equivalent voltage. The matrix expression is given by

$$\bar{\boldsymbol{U}}^+ = (\bar{\boldsymbol{U}} + \bar{\boldsymbol{I}})/2, \quad \bar{\boldsymbol{U}}^- = (\bar{\boldsymbol{U}} - \bar{\boldsymbol{I}})/2 \tag{7}$$

When the network is linear, substituting $\bar{U} = \bar{Z} \cdot \bar{I}$ into Equation (7) yields

$$\bar{\boldsymbol{U}}^- = (\bar{\boldsymbol{Z}} - \boldsymbol{E})(\bar{\boldsymbol{Z}} + \boldsymbol{E})^{-1} \bar{\boldsymbol{U}}^+ \tag{8}$$

In the equation, $\boldsymbol{E}$ is the unity matrix. Establishing the matrix $\boldsymbol{S}$,

$$\boldsymbol{S} = (\bar{\boldsymbol{Z}} - \boldsymbol{E})(\bar{\boldsymbol{Z}} + \boldsymbol{E})^{-1} \tag{9}$$

The expansion form of Equation (6) is

$$\begin{bmatrix} \bar{U}_1^- \\ \bar{U}_2^- \\ \vdots \\ \bar{U}_n^- \end{bmatrix} = \begin{bmatrix} S_{11} & S_{12} & \cdots & S_{1n} \\ S_{21} & S_{22} & \cdots & S_{2n} \\ \vdots & \vdots & \ddots & \vdots \\ S_{n1} & S_{n2} & \cdots & S_{nn} \end{bmatrix} \begin{bmatrix} \bar{U}_1^+ \\ \bar{U}_2^+ \\ \vdots \\ \bar{U}_n^+ \end{bmatrix} \tag{10}$$

where $\boldsymbol{S}$ is known as the S-parameter or parameter $\boldsymbol{S}$.

C. S-Parameters of EMI Filter

Characterizing an EMI filter as a linear passive is reasonable only under the condition of small-signal excitation. Fig. 4 shows the test setup for an EMI filter, which is characterized in terms of waves. Moreover, nonlinear characteristics can be simulated by adding small-signal excitation to the DC bias.

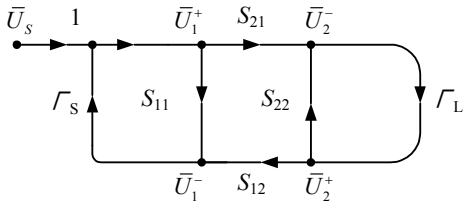

Fig. 5. Scattering parameter signal flow of EMI filter.

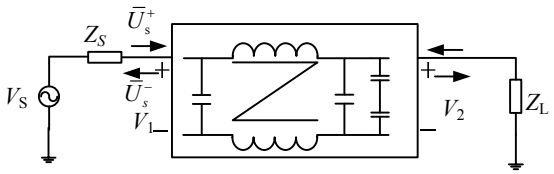

Fig. 6. Single port model of EMI filter.

From the normalized port voltage definition and Equations (1) and (2), the port voltages and currents of two port networks can be derived as

$$V_k = \sqrt{Z_0}(\bar{U}_k^+ + \bar{U}_k^-) \tag{11}$$

$$I_k = (\bar{U}_k^+ - \bar{U}_k^-)/\sqrt{Z_0} \tag{12}$$

where Z_0 is a positive real number that represents the reference impedance of the ports. According to S-parameter theory and Equation (10), we derive

$$\begin{bmatrix} \bar{U}_1^- \\ \bar{U}_2^- \end{bmatrix} = \begin{bmatrix} S_{11} & S_{12} \\ S_{21} & S_{22} \end{bmatrix} \begin{bmatrix} \bar{U}_1^+ \\ \bar{U}_2^+ \end{bmatrix} \tag{13}$$

When reflected to the noise source or load side, $\bar{U}_1^-$ and $\bar{U}_2^-$ will also be reflected to the opposite position because of mismatched impedances. The reflection coefficients, Γ_S at source side and Γ_L at load side, are given by [15]

$$\Gamma_S = (Z_S - Z_0)/(Z_S + Z_0) \tag{14}$$

$$\Gamma_L = (Z_L - Z_0)/(Z_L + Z_0) \tag{15}$$

The current of the circuit in Fig. 4 is characterized by the signal flow graph shown in Fig. 5.

Figs. 5 and 6 show that $\bar{U}_s^-$ represents the normalized voltage wave, which is emitted by the noise source. $\bar{U}_s^+$ and $\bar{U}_s^-$ are the normalized incident and normalized reflection voltage waves of the source port. For the EMI filter, when the impedance Z_S of noise source is determined, the normalized voltage wave is given by

$$\bar{U}_s^+ = \frac{V_1 + I_1 Z_0}{2\sqrt{\left|\mathrm{Re}(Z_0)\right|}} = \frac{V_1 + I_1 Z_0}{2\sqrt{Z_0}} \tag{16}$$

$$\bar{U}_s^- = -\frac{V_1 - I_1 Z_0}{2\sqrt{\left|\mathrm{Re}(Z_0)\right|}} = -\frac{V_1 - I_1 Z_0}{2\sqrt{Z_0}} \tag{17}$$

$$I_1 = V_S/(Z_S + Z_0) \tag{18}$$

According to Equation (1),

$$\bar{U}_s = \bar{U}_s^{+} + \bar{U}_s^{-} \tag{19}$$

$$\bar{U}_S = \sqrt{Z_0} V_S / (Z_S + Z_0) \tag{20}$$

After measuring the *S*-parameter, the Mason formula and signal flow diagram can be used to deduce $\bar{U}_1^{+}$, $\bar{U}_1^{-}$, $\bar{U}_2^{+}$, and $\bar{U}_2^{-}$. According to Equations (9) and (10), the port voltage and current are further calculated.

The ultimate goal of the EMI filter is to control the noise energy transmitted to the load side under a certain standard. Extracting the load-side power is important. According to *S*-parameter theory, the normalized power of the load side is [14]

$$P_L = P_{IN} - P_{REF} = \left|\bar{U}_2^{-}\right|^2 - \left|\bar{U}_2^{+}\right|^2 = \left|\bar{U}_2^{-}\right|^2 (1 - \left|\Gamma_L\right|^2) \tag{21}$$

By using the Mason formula to analyze Fig. 5, we determine that

$$\bar{U}_2^{-} = S_{21}\bar{U}_S / \Delta \tag{22}$$

where

$$\Delta = 1 - (S_{11}\Gamma_S + S_{21}\Gamma_L S_{21}\Gamma_S + S_{22}\Gamma_L) + S_{11}\Gamma_S S_{22}\Gamma_L \tag{23}$$

$$P_L = \left|S_{21}\bar{P}_S / \Delta\right|^2 (1 - \left|\Gamma_L\right|^2) \tag{24}$$

$\left|\bar{P}_S\right|$ is the normalized power of source port

$$P_S = \left|\bar{P}_S\right|^2 / (1 - \left|\Gamma_S\right|^2) \tag{25}$$

The EMI filter network energy transmission gain is given by

$$G_L = 10\log(P_L / P_S) = \left|S_{21} / \Delta\right|^2 (1 - \left|\Gamma_L\right|^2)(1 - \left|\Gamma_S\right|^2)$$
$$= \frac{\left|S_{21}\right|^2 (1 - \left|\Gamma_S\right|^2)(1 - \left|\Gamma_L\right|^2)}{\left|(1 - S_{11}\Gamma_S)(1 - S_{22}\Gamma_L) - S_{21}S_{12}\Gamma_L\Gamma_S\right|^2} \tag{26}$$

From Equation (26), the energy transmission characteristics of the filter network can be extracted by using the *S*-parameter. Thereafter, the operating characteristics of the network can be expressed. However, *IG* should be further studied because of the differences in the characteristics of transmission gain and *IG*.

D. IG Calculated by S-Parameters

In an actual system, the *IG* under the condition of specific impedance should be accurately obtained. *IG* refers to the ratio of the voltage V_2 (or power P_2) and voltage V_0 (or power P_0) [16]. When the filter is connected between the load and power side, this voltage can be expressed in decibel form (DB). V_2 is the load voltage when the EMI filter is placed between the load and source side, whereas V_0 refers to the voltage without the filter.

$$IG = 20\log(V_2 / V_0)$$
$$= 20\log\left[V_2(1 + Z_S / Z_L) / (V_1 + I_1 Z_S)\right] \tag{27}$$

According to Equations (11) and (12)

TABLE I

STRUCTURE PARAMETERS OF PLANAR EMI FILTER

Core	P43	
LC unit	Turns	4
	Thickness	0.8 mm
	Substrate permittivity	500
DM capacitor	Turns	3
	Thickness	0.8 mm
	Substrate permittivity	2000

$$V_1 = \sqrt{Z_0}(\bar{U}_1^{+} + \bar{U}_1^{-}) \tag{28}$$

$$V_2 = \sqrt{Z_0}(\bar{U}_2^{+} + \bar{U}_2^{-}) \tag{29}$$

$$I_1 = (\bar{U}_1^{+} - \bar{U}_1^{-}) / \sqrt{Z_0} \tag{30}$$

$$IG = 20\log\left[\frac{(\bar{U}_2^{+} / \bar{U}_S + \bar{U}_2^{-} / \bar{U}_S)(1 + Z_S / Z_L)}{\bar{U}_1^{+}(1 + Z_S / Z_0) / \bar{U}_S + \bar{U}_1^{-}(1 - Z_S / Z_0) / \bar{U}_S}\right] \tag{31}$$

According to the Mason formula,

$$\bar{U}_2^{+} / \bar{U}_S = S_{21}\Gamma_L / \Delta \tag{32}$$

$$\bar{U}_1^{+} / \bar{U}_S = (1 - S_{22}\Gamma_L) / \Delta \tag{33}$$

$$\bar{U}_1^{-} / \bar{U}_S = [S_{11}(1 - S_{22}\Gamma_L) + S_{21}\Gamma_L S_{21}] / \Delta \tag{34}$$

$$IG = 20\log\left[\frac{S_{21}(1 - \Gamma_L\Gamma_S)}{(1 - S_{11}\Gamma_S)(1 - S_{22}\Gamma_L) - S_{21}S_{12}\Gamma_L\Gamma_S}\right] \tag{35}$$

From (14) and (15), when the Γ_S and the Γ_L are equal to zero, the source and load impedances are in a matching state. Therefore, S_{21} in Equation (35) is the *IG*. However, when the impedances are mismatched, the reflection parameters Γ_S and Γ_L can be calculated to improve EMI filter design.

For switching power supply, determining the hardware circuit enables the noise impedance Z_S of the loop to be obtained through analysis and testing. The load impedance Z_L of the EMI filter is the input impedance of the former device or the standard impedance, which is provided by LISN. S_{11}, S_{21}, S_{12}, and S_{22} can be measured by using an S-parameter tester (Agilent 87511A). The *S*-parameter tester has a calibration function, and its attenuation can be isolated from the noise and energy of the measuring line. Without short-circuit and open-circuit, the *S*-parameter test values are more precise compared with the impedance test values of |*Y*| |*Z*| parameters in the high frequency.

III. TESTING *S*-PARAMETERS AND INSERTION GAIN OF EMI FILTER

This study uses a typical planar EMI filter structure composed of the integrated capacitance of differential mode, leakage inductance layer, integrated LC unit, and magnetic core. Fig. 1 shows the electrical configuration. Table I presents the parameters of the basic cell structure.

The test apparatus uses the Agilent 4395A and Agilent 87511A network analyzer to test the *S*-parameters of the DM and CM structures in the planar filter, respectively. Taking

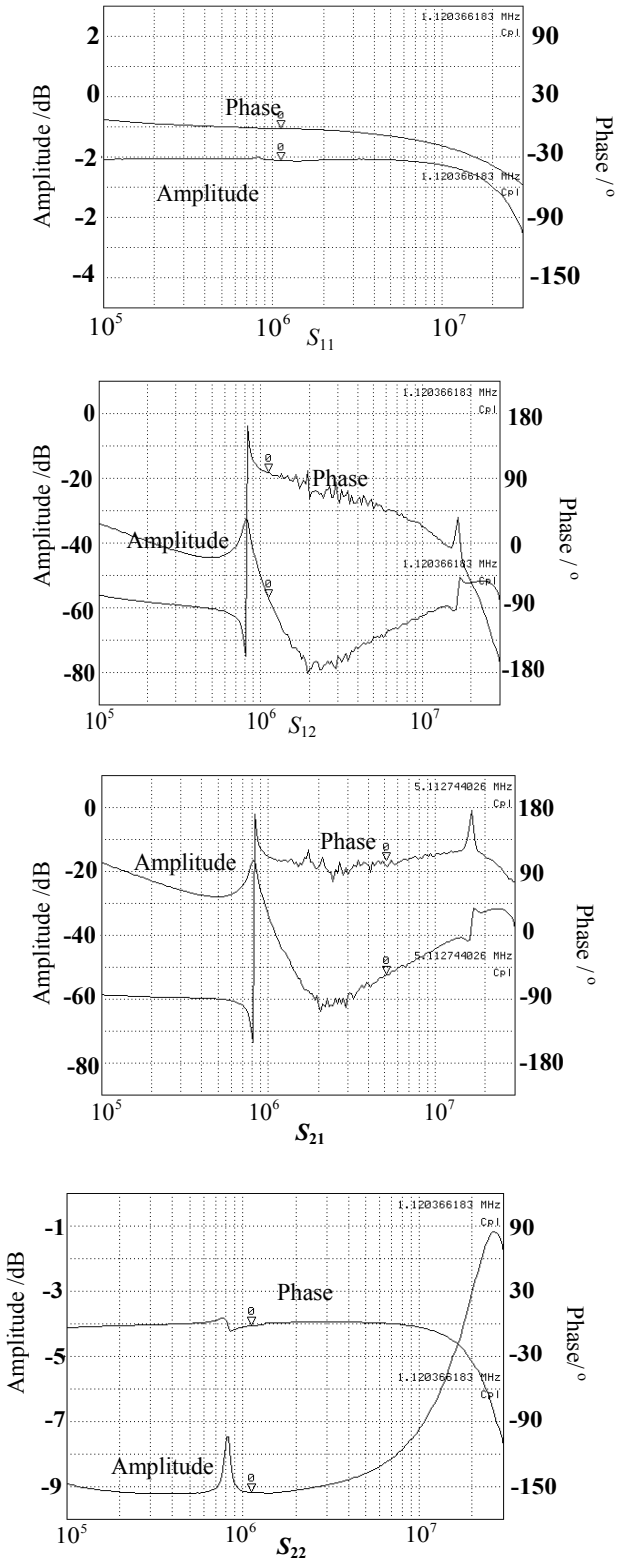

Fig. 7. Test curves of S parameters for DM filter.

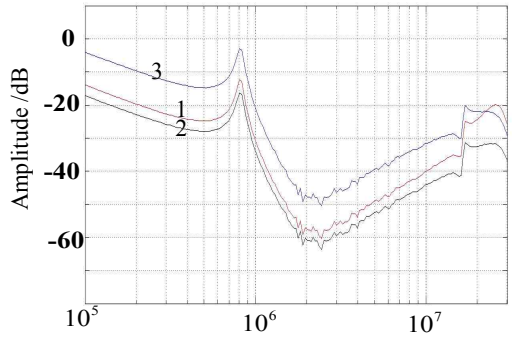

Fig. 8. Comparison of *IG* with different impedances.

1 Z_S=50Ω, Z_L=50Ω
2 Z_S=10kΩ, Z_L=50Ω
3 Z_S=10Ω, Z_L=100Ω

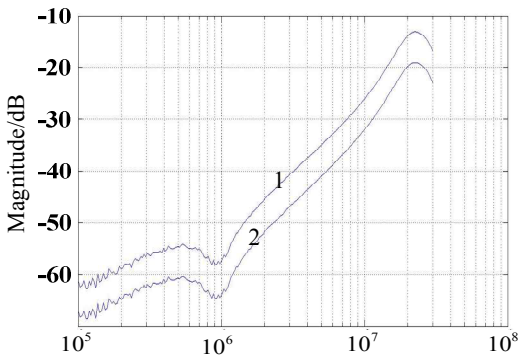

Fig. 9. Calculated curve of *IG* for CM filter.

1—Z_S=50Ω, Z_L=50Ω
2—Z_S=1nF, Z_L=10Ω

the DM structure as an example, Fig. 7 shows the amplitude-frequency and phase-frequency curves of the *S*-parameters.

Fig. 8 clearly shows that when noise source and load impedances are changed, the influence of the different impedance characteristics of *IG* must be considered to optimize the planar EMI filter design.

To calculate the *IG*, the Agilent 4395A Impedance Analyzer is used to test the *S*-parameters of the CM structure. Fig. 9 shows the calculated curve. Subsequently, the signal generator, voltmeter, LISN, EMI filter, and EUT are used to establish the test circuit. The voltages before or after adding the EMI filter are determined by using the voltmeter. The real in-circuit attenuation of several frequency points are then derived (Table II).

A comparison of the *IG* values of curve 2 in Fig. 9 and in Table II reveals that the actual test value coincides with that calculated in the multiple frequency point. In Equation (35), the noise source impedance uses the ideal capacitor impedance curves. Thus, the calculated results are not fully consistent with the test results. Several errors can be assumed between the measured and calculated values.

TABLE II

TEST IG FOR CM FILTER

frequency/MHz	0.500	0.700	1.01	2.10
IG/dB	-59.5	-60.3	-63	-51.2

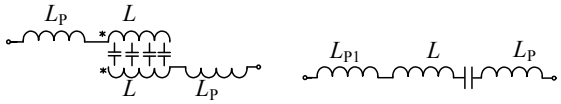

(a) LC series resonant connection.

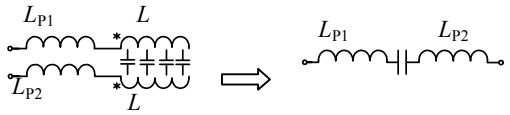

(b) two-port connection.

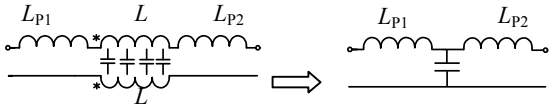

(c) four-port connection.

Fig. 10. Three kinds of connection for integrated LC units.

IV. EXTRACTION OF NEAR-FIELD COUPLING PARAMETERS IN A PLANAR FILTER BY USING *S*-PARAMETER

A. Coupling Parameters of Near-Field for Planar EMI Filter Structure

The high-frequency parameters of a planar filter differ from that of discrete structures. The traditional model (high-frequency parasitic mutual inductance) is no longer applicable. Under certain conditions, the planar filter units can be regarded as an integrated LC structure. Therefore, the use of different connecting methods will affect the equivalent series inductance (ESL) of the integrated capacitor, as shown in Fig. 10.

In Fig. 8, L_{P1}, L_{P2} are the line inductances, whereas L is the planar LC unit inductance.

To reduce the integrated capacitor ESL and to form a complete EMI filter, the integrated LC unit uses the connection method shown in Fig. 10(c). In the EMI filter frequency, the near-field coupling parameters can be used to express mutual inductance. Without considering the coupling parameters with negligible effect, the near-field coupling parameter model of the DM structure in the planar filter is as (Fig. 11).

Fig. 11 shows that L_{P1}, L_{P2} are the input and output inductances of the wire loop, respectively; and L_{P3}, L_{P4} are the inductances between the interior units of the planar filter. L_{P3}, L_{P4} are significantly less than L_{P1}, L_{P2}. Moreover, the coupling effect can be disregarded because of the extreme closeness of

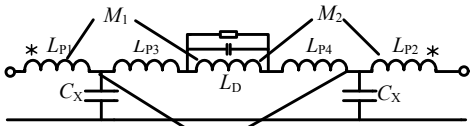

Fig. 11. Near-field coupling M_3 of DM structure.

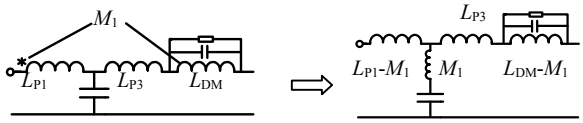

Fig. 12. Calculated M_1 through equivalent capacitor branch.

the LC units in terms of space position. Meanwhile, M_1, M_2 are equal because of the symmetrical electrical and mechanical structures of the planar EMI filter.

B. Use of S-Parameter to Extract Mutual Inductance

To extract the M_1, M_2, a CM inductor and differential capacitor are removed from the core. Fig. 12 shows the equivalent two-port network model.

According to Fig. 12, M_1 is given by

$$M_1 = \sqrt{1/4\pi^2 f^2 C} \tag{29}$$

where f is the resonant frequency of the capacitor branch.

For the extraction of M_3, the CM inductance and retained LC unit constituted by DM capacitance should be removed. Fig. 13 shows the high-frequency model.

Figs. 12 and 13 shows that for any value of mutual inductance, the functional relationship is shown in Fig. 14 after extracting amplitude and phase of the impedance of each branch in corresponding T-transmission network equivalent circuit.

According to microwave network theory, further extraction of mutual inductance parameters results in the conversion of the *S*-parameters into T-transmission network parameters. The relationships of the each branch impedance with the *S*-parameters of the T-network (Fig. 14) are given by

$$Z_1 = \frac{Z_0(1 - S_{22} - S_{22}S_{11} + S_{11} - 2S_{21} + S_{21}^2)}{(1 - S_{22} + S_{22}S_{11} - S_{11} - S_{21}^2)} \tag{30}$$

$$Z_2 = \frac{Z_0(1 + S_{22} - S_{22}S_{11} - S_{11} - 2S_{21} + S_{21}^2)}{(1 - S_{22} + S_{22}S_{11} - S_{11} - S_{21}^2)} \tag{31}$$

$$Z_3 = \frac{2Z_0 S_{21}}{(1 - S_{22} + S_{22}S_{11} - S_{11} - S_{21}^2)} \tag{32}$$

C. Experiments

Table 1 shows the parameters of the planar filter. Fig. 11 shows the M_1, M_2, and M_3 extracted by using Agilent 4395A. The near-field coupling model is created (Fig. 15). Fig. 16

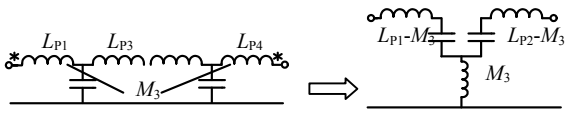

Fig. 13. Calculation of M3 through equivalent circuit.

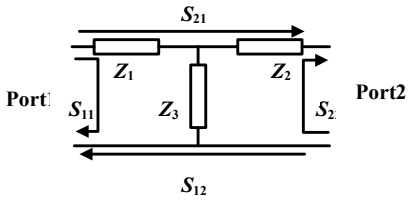

Fig. 14. *S*-parameters of T-network.

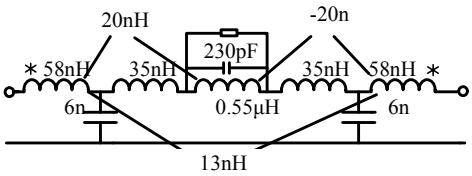

Fig. 15. Parameters for the near-field coupling model.

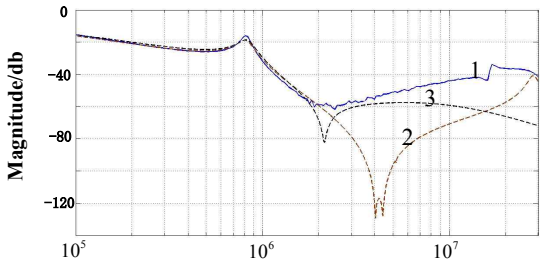

Fig. 16. *IG* for planar EMI filter.

shows the *IG* test values of the differential-mode structure and the model simulation.

Fig. 16 shows that curve 1 represents the *IG* of the differential structure in the planar filter. Curve 2 is the calculation curve of the traditional differential structure, which only considers its own parasitic parameters. Curve 3 represents the *IG* of high frequency model when the near field coupling effect is considered. A comparison of the three curves reveal that the calculation values of the two models are extremely close to their test values in the low-frequency band. However, in the high-frequency band after 2M, the calculation curve of *IG* with near-field coupling is closer to the measurement curve than to the curve of the traditional differential structure model. Therefore, the near-field coupling model is better than the traditional differential model. Meanwhile, the *S*-parameters M_1, M_2, and M_3 are more suitable for the planar EMI filter.

V. CONCLUSIONS

A method using *S*-parameters to characterize EMI filters is discussed. A simplified EMI filter model is proposed to help understand the transmission characteristics of the ports. Meanwhile, the *IG* is developed to predict the filter performance.

The *S*-parameter can be used to extract the near-field coupling parameters. Therefore, establishing an effective near-field parameter model is possible. Compared with the traditional model, which only considers parasitic parameters, the near-field coupling model can predict the characteristics of planar EMI filter more accurately.

ACKNOWLEDGMENT

This study is supported by the Power Electronics Science and Education Development Program of Delta Environmental & Educational Foundation; National Natural Science Foundation of China; Jiangsu Province University Outstanding Science and Technology Innovation Team Project.

REFERENCES

[1] R. L. Ozenbaugh, *EMI Filter Design*, Taylor & Francis, 2nd ed., 2001.
[2] S. Wang and Chenchen Xu, "Design theory and implementation of planar EMI filter based on annular integrated inductor-capacitor unit," *IEEE Trans. Power Electron.*, Vol. 28, No. 3, pp. 1167-1175, Mar. 2013.
[3] H. Hsieh, J. Li, and D. Chen, "Effects of X capacitors on EMI filter effectiveness," *IEEE Trans. Ind. Electron.,* Vol. 55, No. 2, pp. 949-955, Feb. 2008.
[4] H. Huang and L. Deng, "Improving the high-frequency performance of integrated EMI filter with multiple ground layers," *Asia-Pacific Symposium on Electromagnetic Compatibility*, pp. 249-252, 2012.
[5] J. Drinovsky, J. Svacina, and P. Bednar, "Operation amplifiers in EMI filter insertion loss measurement setup," *Radioelektronika, 17th International Conferences,* pp. 1-3, Apr. 2007.
[6] S. Wang, F. C. Lee, and W. G. Odendaal, "Characterization and parasitic extraction of EMI filters using scattering parameters," *IEEE Trans. Power Electron.*, Vol. 20, No. 2, pp. 502-510, Mar. 2005.
[7] W. Chen, L. Feng, H. Chen, and Z. Qian, "Near field coupling effects on conducted EMI in power converter," *in 37th IEEE Power Electronics Specialists Conference*, *PESC '06*, pp. 252-259, 2006.
[8] S. Wang and F. C. Lee, "Using scattering parameters to characterize EMI filter," *in 35th IEEE Annual Conference on Power Electronics Specialists Conference,* pp. 297-303, 2004.
[9] V. Tarateeraseth, K. Y. See, F. G. Canavero, and R. W. Chang, "Systematic electromagnetic interference filter design based on information from in-circuit impedance measurements," *IEEE Trans. Electromagn. Compat.,* Vol. 52, No. 3, pp. 588-598, Aug. 2010.
[10] J. Espina, J. Balcells, A. Arias, C. Ortega, and N. Berbel, "EMI model of an AC/AC power converter," *Vehicle Power and Propulsion Conference (VPPC)*, pp. 1-6, 2010.

[11] J. Pleite, R. Pietro, R. Asensi, J. A. Cobos, E. Olias, "Obtaining a frequency-dependent and distributed-effects model of magnetic components from actual measurements," *IEEE Trans. Magn.,* Vol. 35, No.6, pp. 4490-4502, Nov. 1999.
[12] J. Drinovsky, J. Svacina, M. Zamazal, T. Urbanec, and J. Lacik, "Variable impedance in measuring EMI filter's insertion loss," *Communications, Asia-Pacific Conference on*, pp. 24-27, 2005.
[13] D. M. Pozar, *Microwave Engineering*, John Wiley & Sons, Inc, 1998.
[14] L. Besser and R. Gilmore, *Practical RF Circuit Design for Modern Wireless Communication Systems*, Artech House Publishers, pp. 31-49, 2006.
[15] S. Wang, F. C. Lee, and W. G. Odendaal, "Characterization and parasitic extraction of EMI filters using scattering parameters," *IEEE Trans. Power Electron.*, Vol. 20, No. 2, pp. 502-510, Mar. 2005.
[16] D. Zhang, D. Y. Chen, and D. Sable, "A new method to Characterize EMI Filter," *Applied Power Electronics Conference and Exposition,* Vol. 2, pp. 929-933, 1998.

Shishan Wang was born in Shaanxi Province, China, in 1967. He received his Ph. D in Electrical Engineering in 2003 from Xi'an Jiaotong University, China. He is currently working at Nanjing University of Aeronautics and Astronautics in the Department of Electrical Engineering. His research interests include the electromagnetic compatibility of power electronic system, electromagnetic numerical calculation, and its application in electrical devices.

Min Gong was born in China in 1989. She received her B.S. in Electrical Engineering degree from Nanjing University of Aeronautics and Astronautics, Nanjing, China, in 2012. At present, she is pursuing an M.S. degree in Electrical Engineering at the same university. Her main research interests include the electromagnetic compatibility of power electronic system.

Chenchen Xu received her B.S. degree in Electrical Engineering and automation from the Anhui University of Technology, Anhui, China, in 2011. At present, she is working to complete her M.S. degree in Electrical Engineering at Nanjing University of Aeronautics and Astronautics, Nanging, China. Her main research interests include electromagnetic compatibility of power electronics, as well as the design and development of a new type electromagnetic interference filter.